Hydrometallurgy, 19 (1987) 227–242
Elsevier Science Publishers B.V., Amsterdam — Printed in The Netherlands

Kinetics and Mechanism of the Oxidative Dissolution of a Zinc Sulphide Concentrate in Ferric Sulphate Solutions

F.K. CRUNDWELL

Council for Mineral Technology (MINTEK), Private Bag X3015, Randburg 2125 (South Africa)

(Received October 31, 1986; accepted in revised form June 5, 1987)

ABSTRACT

Crundwell, F.K., 1987. Kinetics and mechanism of the oxidative dissolution of a zinc sulphide concentrate in ferric sulphate solutions. *Hydrometallurgy*, 19: 227–242.

The kinetics of the oxidative dissolution of a zinc sulphide (sphalerite) concentrate was studied. It was observed that the dissolution of the concentrate continued beyond 90% conversion in two hours at 80°C. The kinetics of dissolution are successfully described by an electrochemical mechanism in which the charge transfer from the solid to the oxidant is rate-limiting. The rate of reaction is proportional to the sum of the concentrations of the $Fe^{3+}(aq)$ and $FeHSO_4^{2+}$ complexes with a reaction order of one-half. The addition of Fe(II) to the solution had an indirect effect on the reaction rate, by decreasing the concentrations of the electro-active ions. Addition of $ZnSO_4$ did not affect the reaction rate.

INTRODUCTION

The rate of dissolution of a solid depends on the processes occurring at the solid–solution boundary. The dissolution processes can be classified on the basis of the rate-determining step, for example mass transport, chemical reaction, or charge transfer [1]. Dissolution reactions can be further classified on the basis of the overall reaction as non-oxidative dissolution, in which no change occurs in the formal oxidation states of the constituent atoms of the solid, or as oxidative or reductive dissolution, in which such a change does occur.

Oxidative dissolution is an important step in the hydrometallurigical extraction of metals from sulphide ores, and considerable attention has been focussed on the development of processes for the leaching of zinc sulphide (sphalerite) in chloride and sulphate solutions [2–14] using dissolved iron,

$$ZnS + 2Fe^{3+} \rightleftharpoons Zn^{2+} + 2Fe^{2+} + S \quad (1)$$

0304-386X/87/$03.50 © 1987 Elsevier Science Publishers B.V.

Although much research work on the dissolution of sphalerite has been reported, most of it was done to demonstrate that sphalerite could be readily dissolved under specific conditions; fundamental studies are rare.

During the past decade the application of the mixed potential reaction mechanism, which is analogous to the corrosion mechanism, has gained acceptance in leaching and flotation research. Sulphide ores are typically semiconductors, and the application of this model to leaching kinetics assumes that the potential across the solid side of the interface (the space-charge region) remains approximately constant, so that the applied potential appears only across the Helmholtz layer. This implies metal-like behaviour, with a charge-transfer coefficient of about one-half. Recently, the mixed potential model was applied to the dissolution of zinc sulphide concentrates [2–4].

Jin and Warren [2] proposed an adsorption electrochemical model for the dissolution of sphalerite in chloride solutions. They observed that, at low concentrations, the rate of reaction is proportional to $[Fe(III)]^{0.5}$ and that, at higher concentrations, the rate becomes independent of [Fe(III)]. The change in Fe(III) dependence occurred at 0.8 *M* Fe(III) for particles of three size ranges. They attributed this to the onset of complete coverage of the surface by ferric ions, and described this in terms of a Langmuir adsorption isotherm in combination with the mixed potential model. Similar one-half dependence results were presented for the addition of Cl^- to the solution. Competitive adsorption onto the same sites by H^+ was not mentioned, and it is not clear how they would account for the effect of the addition of Fe(II) to the leaching solution in their model.

Verbaan and Crundwell [3,4] derived a model in which the mixed potential or corrosion potential, E, can be approximated by the redox potential for the Fe^{3+}/Fe^{2+} couple. The rate of reaction, r is given by

$$r = k \exp(0.5\, FE/RT) \tag{2}$$

where

$$E = E^\circ + (RT/F) \ln ([Fe^{3+}]/[Fe^{2+}]) \tag{3}$$

and 0.5 represents the charge-transfer coefficient. This gives the same one-half order dependence on $[Fe^{3+}]$ at constant [Fe(II)] that was found by Jin and Warren [2]. The combination of this model with shrinking-particle geometry and calculation of the redox potential gave an excellent reproduction of the results of batch leaching.

Verbaan [5] investigated the effect of the concentration of Fe(III) and Fe(II) on the rate of reaction of a sphalerite concentrate at 65 °C in 0.1 *M* H_2SO_4. Equations (2) and (3) indicate that the rate of reaction should display a Nernstian response to variations in [Fe(III)] and [Fe(II)], i.e., a plot of the logarithm of the initial rate against the redox potential should give a slope

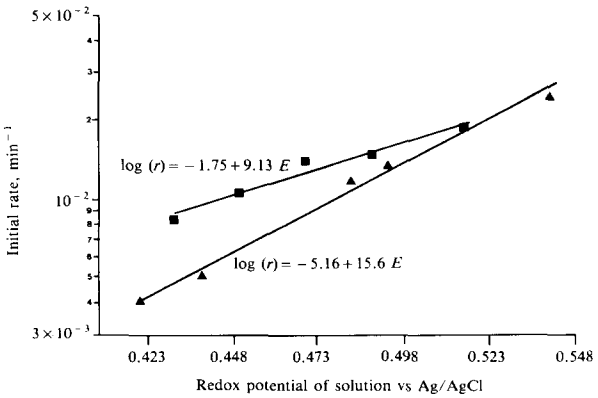

Fig. 1. Correlation of the initial rate of reaction for the ferric sulphate leaching of sphalerite with the measured redox potential (vs. Ag/AgCl) using Verbaan's data [5] in 0.1 *M* H_2SO_4, 65°C. ▲: 0.038 *M* Fe(II), various Fe(III). ■: 0.45 *M* Fe(III), various Fe(II).

of $0.5F/RT$, which has a value of 17.2 V^{-1} at 65°C, corresponding to a Tafel slope of 0.136 V.

The data of Verbaan are presented in Fig. 1, which illustrates that at constant [Fe(II)] and varying [Fe(III)], eqn. (2) is satisfied since the measured slope, 15.6 V^{-1}, is close to the expected 17.2 V^{-1}, but at constant [Fe(III)] and varying [Fe(II)] equation 2 is not satisfied, since the measured slope, 9.1 V^{-1}, is far from the expected 17.2 V^{-1}. The non-Nernstian response of the rate of dissolution with [Fe(II)] at constant [Fe(III)] suggests that the model, represented by eqns. (2) and (3), needs to be examined in more detail.

In any operating plant the concentrations of both Fe(II) and Fe(III) will fluctuate. It is therefore important that the effect of the Fe^{3+}/Fe^{2+} redox couple be understood. This paper extends previous proposals to take the effect of the addition of Fe(II) into account. Extensive results for zinc sulphide dissolution in chlorite solutions have been reported by Jin and Warren [2,6] and Dutrizac and MacDonald [7]. The model developed in this study has been applied to their results to thoroughly demonstrate its value.

EXPERIMENTAL

A sphalerite concentrate from the Gamsberg deposit in South Africa was used in the present study. The concentrate was wet-screened and a sample in the size range −53 +44 μm was selected. This size fraction was washed with Na_2S to remove flotation reagents [6], and then washed in dilute sulphuric acid. The chemical compositions and surface areas are shown in Table 1. Mineralogical analyses were carried out on the sample as received and after it had been leached. The results are shown in Table 2. A microscopic examination of polished sections of the sample revealed a rim of fractured material.

TABLE 1

Chemical compositions of the sphalerite concentrate (all values in %)

Zn	51.0
Fe	9.08
Cu	0.14
Pb	0.74
Mn	2.34
Al	0.35
S^{2-}	28.8
S^0	2.2
Cd	0.087
K	0.136
Mg	0.05
Ca	0.02
Ba	0.015
BET (m^2/g)	0.55

The reactor consisted of a two litre cylindrical glass vessel with a flat stainless-steel impeller driven by a variable speed motor. A single stainless-steel baffle was installed. The temperature was maintained to within 0.5°C by a contact thermometer connected to the heating element. A condenser was connected to one of the ports in the lid. A solution bridge connected a calomel reference electrode to the solution, and the redox potential was measured by use of a platinum electrode. All potentials reported here refer to the saturated calomel electrode (SCE) unless otherwise stated. The redox potential was maintained to within 2 mV by the addition of 3% hydrogen peroxide, the amount of the addition being controlled by a Radiometer PHM84/TTT80 titrator system. The pH of the solution, which was measured with a combined glass and

TABLE 2

Mineralogical compositions of the sphalerite concentrate (all values in %)

	As received	After leaching
Sphalerite — liberated	98.2	14.6
Sphalerite — locked to sulphides	0.6	0.3
Sphalerite — locked to gangue	–	–
Chalcopyrite	–	–
Galena	–	–
Pyrite + pyrrhotite	1.2	0.9
Gangue	–	1.0
Sphalerite + sulphur	–	63.6
Sulphur products	–	19.6

Ag/AgCl reference electrode, was maintained to within a 0.1 pH units in the pH range 1 to 1.5 by the addition of sulphuric acid (500 g/L). The pH was controlled by a similar system to that used for the control of redox potential. Distilled water and analytical reagent grade chemicals were used.

The standard conditions used in this study were 0.5 *M* Fe(III), 0.1 *M* H_2SO_4, 78°C, and 2 g/L concentrate. Once initial conditions had stabilised, 3 g of concentrate was rapidly poured in 1.5 litres of solution. The control systems automatically maintained the pH and redox potential levels. A low solid to liquid ratio was chosen so that the addition of H_2O_2 and H_2SO_4 during reaction would not significantly change the total volume of solution.

Samples of solution were taken during the reaction by use of a 15 mL syringe and filtered immediately under pressure. The concentrations of the zinc and iron in solution were determined by atomic absorption spectrophotometry, and the addition of hydrogen peroxide during the reaction was monitored as a check on the zinc concentrate in solution, and was always found to be stoichiometrically proportional to the zinc concentration. Direct oxidation of the ZnS by H_2O_2 was assumed to be minimal due to the low solid–liquid ratio, and the fast oxidation reaction with Fe(II).

RESULTS AND DISCUSSION

Dissolution kinetics of Gamsberg sphalerite

If it is assumed that a surface reaction controls the rate of dissolution, the shrinking-particle model for spherical geometry has the following form:

$$k_r t = 1 - (1 - X)^{1/3} \qquad (4)$$

where X is the conversion, k_r is a constant, and t is the reaction time elapsed. Typical results collected in the present study are presented in Figs. 2 and 3 as plots of $1 - (1 - X)^{1/3}$ against t. These figures illustrate that, in the initial stages of reaction, the reaction displays linear kinetics, which supports the assumption of surface reaction control. This is followed by diffusion-through-the-product-layer control in the latter stages of reaction. Results similar to those shown in Fig. 2 were obtained for a set of experiments with 0.125 *M* Fe(III) and a similar variation of Fe(II) concentration.

As mentioned earlier, microscopic examination revealed that the Gamsberg material was surrounded by a rim of fractured material. This material dissolved rapidly, resulting in the initial conversion of 0.108 shown in Figs. 2 and 3. The value of k_r in equation (4) was determined by linear regression on the

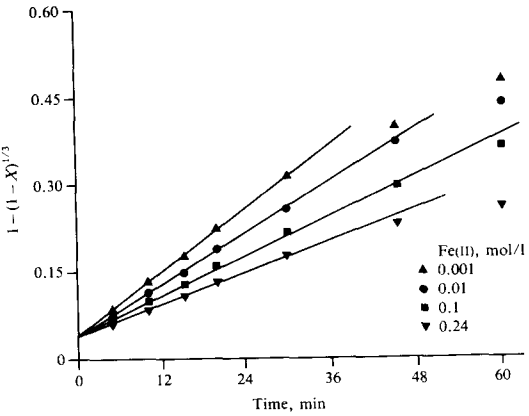

Fig. 2. Dependence of the rate of reaction on the concentration of Fe(II) with 0.51 *M* Fe(III) at 78°C.

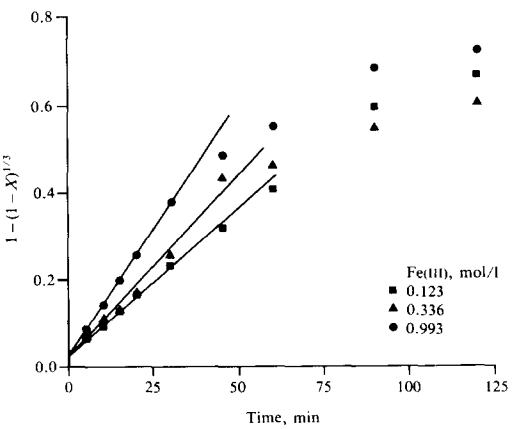

Fig. 3. Dependence of the rate of reaction on the concentration of Fe(III) with 0.0048 *M* Fe(II) at 78°C.

points up to 30 min. The regression was derived so that the intercept corresponded to a conversion of 0.108 for all the runs. The deviation from reaction control is apparent at higher conversions, as a result of the sulphur layer that forms on the particle surface. As this layer increases in thickness, the supply of reactants and the removal of products through the layer becomes limiting, and shrinking-core kinetics are applicable in these regions. Unfortunately, attempts to model the entire reaction curve using mixed-reaction kinetics and fitting the reaction and diffusion parameters were unsuccessful. The incorporation of a pore-blockage mechanism, which is analogous to catalyst deactivation, did not improve the model.

If the model represented by eqn. (2) is correct, then all dissolution reactions at the same redox potential and temperature will have the same rate of reac-

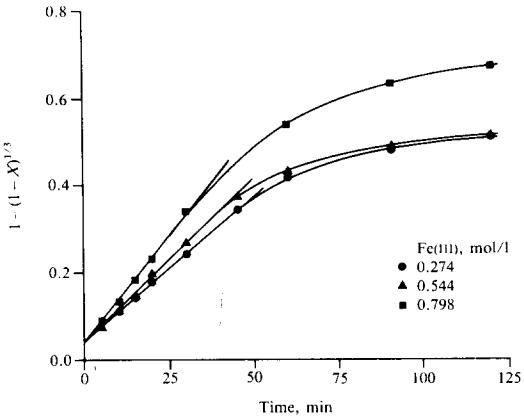

Fig. 4. Dependence of the rate of reaction on the concentration of Fe(III) at a constant redox potential of 575 mV vs. SCE at 78°C.

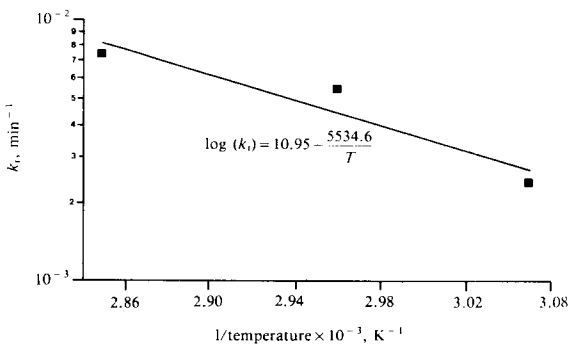

Fig. 5. Arrhenius diagram for the dissolution of Gamsberg sphalerite in ferric sulphate solution.

tion. Figure 4 illustrates three reactions at 575 mV and different concentrations of Fe(III) and Fe(II), showing clearly that this model does not adequately describe the mechanism of reaction. Figures 2 to 4 illustrate that, at high conversions, diffusion through the product layers becomes the dominant mechanism of reactions.

An Arrhenius plot of the reaction rate constant, k_r, is presented in Fig. 5. An activation energy of 46 kJ/mol is obtained, which agrees favourably with that obtained by other researchers [2,5].

The effect of the addition of $ZnSO_4$ to the solution was investigated. The initial rate of reaction was unaffected by zinc concentrations of 0.05 *M* and 0.01 *M*. This result is consistent with previously published results [9,10].

Mechanism of dissolution of Gamsberg sphalerite

The reactions involved in the leaching of sphalerite are undoubtedly electrochemical in nature, the rate of charge transfer across the Helmholtz layer

and the space-charge region being the rate-determining step. Sphalerite cannot be used as an electrode in conventional electrochemical experiments because of its high resistivity. Mixtures of sphalerite and graphite have been used as electrodes [12–15]. The graphite serves to decrease the resistivity, so that the applied potential appears across the Helmholtz layer. However, Scott and Nicol [12] reported that the presence of graphite in contact with sphalerite altered the mechanism of reaction — a fourfold to fivefold increase in the rate of reaction being obtained for a sphalerite–graphite electrode over that of a sphalerite–PTFE electrode. Guerette and Ghali [14] reported similar results, i.e. that the anodic behaviour of compacted sphalerite–graphite mixtures is different from that of uncompacted samples.

In a study of the semiconducting characteristics of galena electrodes, Richardson and O'Dell [16] observed Tafel slopes for anodic oxidation that are consistent with the mechanism for anodic dissolution proposed by Paul et al. [17]:

$$PbS \rightleftharpoons Pb^{2+} + S^- + e^- \tag{5}$$

$$S^- \rightarrow S + e^- \tag{6}$$

Richardson and O'Dell [16] reported that, at potentials corresponding to the Tafel region for anodic oxidation, the surface photovoltage was saturated, suggesting that the Fermi energy at the surface is very near to, or pinned at the conduction-band edge. Further changes in the electrode potential in the anodic direction would then occur primarily across the Helmholtz layer, and metal-like behaviour would be observed. They considered that this also accounts for the insensitivity of anodic dissolution to illumination.

Sphalerite is a semiconductor with a wide band gap (3.6 eV) and high resistivity (10^7 to 10^9 ohm cm). The iron content in the sphalerite has the effect of narrowing the band gap energy (0.49 eV for 12 atom-% Fe) and supplying holes by a hole-hopping mechanism in a d-orbital impurity band [18]. (Band gap narrowing is indicative of semiconductor degeneracy and metal-like behaviour.) Transfer of electrons at the semiconductor/electrolyte interface is dominated by the interaction with this iron impurity band, and a linear increase in rate of reaction is found with sphalerite iron content [11]. This rate of charge transfer is described by the Butler–Volmer equation.

It is not unreasonable to assume that the results observed by Richardson and O'Dell [16] and Paul et al. [17] can be applied to Gamsberg sphalerite. Reactions that are limited by charge transfer at the surface are quantitatively described by the Butler–Volmer equation, which relates the current density, i, to the potential across the Helmholtz layer, $\Delta\phi$. In the anodic potential region, the anodic dissolution current for reactions (5) and (6) is given by Paul et al. [17] as:

$$i_A = 2k_{5A}F\exp((1-\beta_{5A})\Delta\phi F/RT) \quad (7)$$

where $\Delta\phi$ is the potential across the mineral surface, β_{5A} is the charge-transfer coefficient, F is Faraday's constant, and k is the rate constant. The other symbols have their usual significance.

The presence of dissolved iron in solution contributes to the kinetics by the redox couple:

$$Fe^{3+} + e^- \rightleftharpoons Fe^{2+} \quad (8)$$

for which the net anodic current density, i_{Fe}, is given by:

$$i_{Fe} = F k_{8A}[Fe^{2+}]\exp((1-\beta_8)\Delta\phi F/RT) - Fk_{8C}[Fe^{3+}]\exp(-\beta_8\Delta\phi F/RT) \quad (9)$$

The concentration of oxidant and reductant in eqn. (9), and therefore in the following eqns. (10) to (14), can represent any, or all of, the ionic species present in solution. Since no net current flows during the dissolution of a particle, the following expression is obtained:

$$0 = i_A + i_{Fe} \quad (10)$$

$$0 = 2k_{5A}\exp((1-\beta_{5A})\Delta\phi F/RT) + k_{8A}[Fe^{2+}]\exp((1-\beta_8)\Delta\phi F/RT) - k_{8C}[Fe^{3+}]\exp(-\beta_8\Delta\phi F/RT) \quad (11)$$

The role of the iron couple can be divided into three regions, as follows:

Case (*i*): The partial anodic current due to the oxidation of Fe(II) is negligible.

$$i_A = F(2k_{5A})^{\alpha}\ (k_{8C}[Fe^{3+}])^{\delta} \quad (12)$$

$$\alpha = \beta_8/(1-\beta_5+\beta_8)$$

$$\delta = (1-\beta_5)/(1-\beta_5+\beta_8)$$

Case (*ii*): The partial anodic currents due to the oxidation of Fe(II) and ZnS are significant

$$i_A = 2Fk_{5A}\{(k_{8C}[Fe^{3+}]/(2k_{5A}+k_{8A}[Fe^{2+}])\}^{0.5} \quad (13)$$

Case (ii) assumes that the β values are equal.

Case (*iii*): The partial anodic current due to the oxidation of ZnS is negligible compared to that due to the oxidation of Fe(II).

$$i_A = 2Fk_{5A}(k_{8C}[Fe^{3+}]/k_{5A}[Fe^{2+}])^{\delta} \quad (14)$$

$$\delta = 1-\beta_5$$

Cases (ii) and (iii) represent the reversible Fe^{3+}/Fe^{2+} couple used in the previous model, eqn. (2). Figures 1 and 4 show that this is inadequate as a description of the leaching characteristics. However, the concentration of the oxidant in solution is dependent on the ionic equilibria, and the concentrations

TABLE 3

Iron stability constants at zero ionic strength

Equation	Stability constant	Source Ref.
$Fe^{3+}+SO_4^{2-}+H^+ \rightleftharpoons FeHSO_4^{2+}$	$\exp(33.334-7629.9/T)$	[19]
$Fe^{3+}+SO_4^{2-} \rightleftharpoons FeSO_4^+$	$\exp(-900+39110.9/T+136.61\log(T))$	[19]
$Fe^{2+}+SO_4^{2-} \rightleftharpoons FeSO_4$	$10^{(3.339-337.37/T)}$	[19]
$Fe^{2+}+SO_4^{2-}+H^+ \rightleftharpoons FeHSO_4^+$	$\exp(30.69-7290.4/T)$	[19]
$Zn^{2+}+SO_4^{2-} \rightleftharpoons ZnSO_4$	$10^{2.38}\exp(1.067-318.2/T)$	[21]
$H^+ + SO_4^{2-} \rightleftharpoons HSO_4^-$	$\exp(-14.0321+2825.2/T)$	[22]

of the various species in solution were calculated to investigate this aspect of the dissolution process.

The redox potential, given by eqn. (3), is a measure of the activity ratio of the Fe^{3+} and Fe^{2+} ions (or any other redox couple formed by ferric and ferrous sulphate complexes) in a mixed electrolyte. Dry [19] was able to calculate the Fe^{3+}/Fe^{2+} redox potential in the ionic strength range 0 to 4 and in the temperature range 22 to 90 °C, by accounting for the following complexes in solution: $FeSO_4^+$, $FeHSO_4^{2+}$, $FeSO_4$, $FeHSO_4^+$, and HSO_4^-. Dry used the Debye–Hückel equation, in which the real rather than the formal ionic strength was substituted, to estimate the individual activity coefficients of the ions in solution, and used Pitzer et al.'s correlation [22] to estimate the dissociation of HSO_4^- at the solution ionic strength. He selected values of the stability constants of the complexes at zero ionic strength from within the range of values reported in the literature so as to optimize the difference between the measured and calculated redox potentials. The values of these constants are given in Table 3. The use of the Debye–Hückel equation is justified in this calculation for concentrations up to 0.5 M [27].

The numerical procedure described by I and Nancollas [20] was used in the present study in conjunction with Dry's stability constant data for the calculation of the concentrations of the iron sulphate species. $FeSO_4^+$ is the dominant species in solution (approximately 85%) at the leaching conditions, followed by $FeHSO_4^{2+}$ (10 to 15%). The concentration of the ferric aquo-ion is very low. The distribution of the iron species in solution is shown in Fig. 6. The root mean square deviation $S(E)=\sqrt{1/(N-1)\Sigma((E_{cal}-E_{exp})/E_{exp})^2}$ of the measured and calculated redox potentials is less than 2.0% for the initial conditions for all the experiments in this study. It is concluded that since the redox potential is accurately calculated, this presents a reliable procedure for the calculation of the activities and concentrations of the complexes in solution.

An examination of Fig. 1 suggests that the addition of ferrous sulphate does

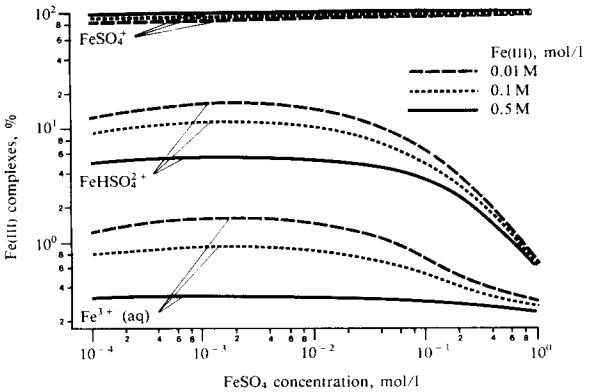

Fig. 6. The distribution of the Fe(III) species in solution in 0.1 *M* H_2SO_4 at 78°C.

not directly affect the rate of leaching, i.e. the iron couple is not reversible at the sphalerite surface, and case (i) conditions apply. Correlation of the rate with the $FeSO_4^+$ complex did not yield satisfactory results for this model.

However, Fig. 7 shows close correlation of the rate of dissolution with the sum of the concentrations of Fe^{3+} (aq) and $FeHSO_4^{2+}$ for the data shown in Fig. 1. This figure is a plot of the case (i) model assuming that the $FeSO_4^+$ complex is inactive at the sphalerite surface. The success of this assumption indicates that the Fe^{3+} (aq) and $FeHSO_4^{2+}$ are the electro-active species at the sphalerite surface. The slope of the best fit through these points is 0.45. This gives a Tafel slope of 0.122 V, significantly close to the expected value of 0.136 V.

Figure 8 is a similar diagram for all the experimental results obtained for the Gamsberg sphalerite at 78°C. The slope for these results is 0.54, which gives a Tafel slope of 0.150 V. This is again close to the expected Tafel slope of 0.140 V. The close correlation of these results with the case (i) model demonstrates that the effect of the addition of Fe(II) to the solution is indirect, in that Fe(II) sulphate changes the concentrations of the electro-active species in solution, and hence affects the rate of dissolution. The Fe^{3+}/Fe^{2+} couple in sulphate solutions is therefore irreversible at the Gamsberg surface. Parker et al. [23] argued a similar case for the behaviour of a chalcopyrite electrode in iron sulphate solutions, and noted that the Fe^{3+}/Fe^{2+} couple in chloride is reversible at the chalcopyrite surface, increasing the rate of reaction.

The dependence of the rate on particular complexes in solution is explicable in terms of the factors controlling the solution complexes. $FeSO_4^+$ is described by Ashurst and Hancock [24] as an inner-sphere complex, whereas $FeSO_4$, $FeHSO_4^{2+}$ and $FeHSO_4^+$ are outer-sphere complexes (ion pairs). Charge transfer to $FeSO_4^+$ would require the breaking of the Fe^{3+} and SO_4^{2-} bond in

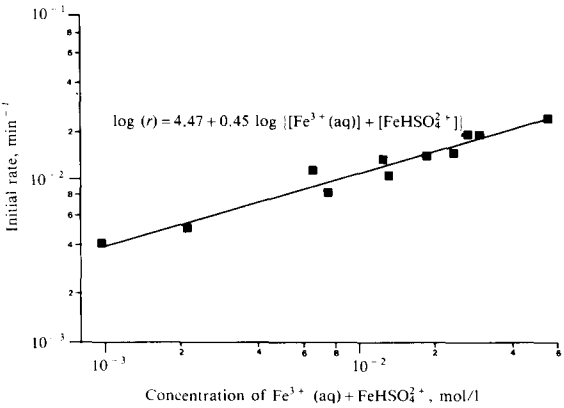

Fig. 7. Case (i) model for data presented by Verbaan [5] (Fig. 1) assuming that $FeSO_4^+$ is inactive.

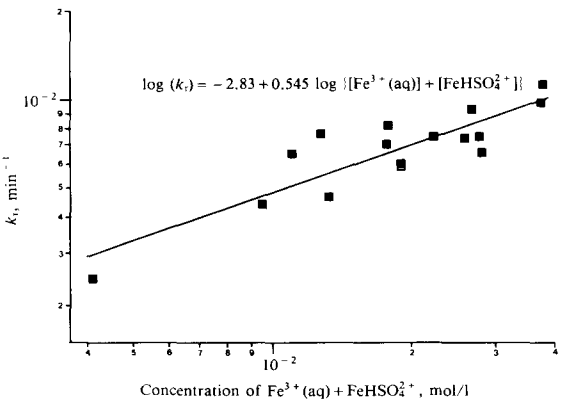

Fig. 8. Case (i) model for the leaching of Gamsberg sphalerite assuming $FeSO_4^+$ is inactive for data from Figs. 2–4.

the inner coordination sphere to form the $FeSO_4$ outer-sphere complex. Therefore, charge transfer to $FeSO_4^+$ is retarded due to the different bonding in the $FeSO_4^+$ and $FeSO_4$ complexes, and the outer-sphere couples [$FeHSO_4^{2+}/FeHSO_4^+$ and $Fe^{3+}(aq)/Fe^{2+}(aq)$] are the electro-active species.

Leaching of sphalerite in ferric chloride solutions

Dutrizac and MacDonald [7] reported that the addition of Fe(II) to the ferric chloride leaching solution has a direct effect on the rate of dissolution. If this is the case, then the Fe^{3+}/Fe^{2+} couple can be regarded as being reversible at the sphalerite surface in chloride solutions, and the potential difference across the Helmholtz layer is dominated by this couple. A plot of the rate constant against the $FeCl_2$ concentration on a logarithmic scale for their data [7]

indicates that two distinct regions exist, corresponding to case (i) conditions (rate independent of $[FeCl_2]$) at low $FeCl_2$ concentrations ($<0.4\,M$) and case (iii) conditions at higher $FeCl_2$ concentrations ($>0.4\,M$).

Dutrizac and MacDonald [7] observed that the rate was proportional to $[Fe(III)]^{0.36}$. The concentrations of the ferric and ferrous species in solution were calculated from stability constants given by Ashurst and Hancock [24] and Butler [25] using the same calculation procedure as that for the sulphate solutions. The rate was proportional to $[FeCl^{2+}]^{0.42}$ and $[FeCl_2{}^{+}]^{0.31}$, which gives an overall reaction order of 0.36. Jin and Warren [2] reported a reaction rate proportional to $[Fe(III)]^{0.5}$, and the reaction order of both $FeCl^{2+}$ and $FeCl_2{}^{+}$ was 0.5. Therefore, the charge transfer in chloride solutions is not dominated by a particular ionic species as it is in sulphate solutions.

Jin and Warren [2] reported a change in the dependence of the reaction on Fe(III) chloride concentration from one-half order to zero order. They proposed that this was due to onset of complete coverage and described this using the Langmuir isotherm. An ion in aqueous solutions becomes solvated, the significance of which is that such ions are seldom adsorbed at the semiconductor surface or at the inner Helmholtz plane (IHP). Solvated ions, such as $Fe^{3+}(aq)$, are adsorbed electrostatically at the outer Helmholtz plane (OHP), which is not identical to specific site adsorption. The change of reaction order could be indicative of the anodic current density for zinc sulphide, given by eqn. (7), reaching a limiting value, due to a diffusion-limited supply of solid-phase interaction. Therefore, for Fe(III) concentrations above 0.8 *M*, an increase in the Fe(III) concentration will not result in an increase in the rate of dissolution, and the reaction dependence changes to zero order. This change in dependence was not observed by Dutrizac and MacDonald [7], although they covered a larger Fe(III) concentration range than Jin and Warren [2]. The differences in these observations are probably a consequence of the different sphalerites studied. Dutrizac and MacDonald [7] used a pure natural sample, while Jin and Warren [2] used an impure concentrate. Zero order dependence could possibly be observed at higher Fe(III) concentrations for Dutrizac and MacDonald's material. Further investigation of this feature is needed.

The effect of the chloride ion is twofold: increasing the concentration of Cl^- decreases the potential of the Fe^{3+}/Fe^{2+} redox couple, and contact adsorption at the inner Helmholtz plane is often observed for Cl^- ions. A dependence on Cl^- for non-oxidative dissolution has been reported, and explained in terms of the formation of complexes of Zn^{2+} and Cl^- [26]. The removal of zinc lattice ions, Zn_l, may be coupled with the complexing of chloride ions, according to

$$Zn_l + nCl^- \rightarrow ZnCl_n^{2-n} \tag{15}$$

for which eqn. (7) may be rewritten as

$$i_A = 2k_{5A}[Cl^-]^n F \exp((1-\beta_{5A})\Delta\phi F/RT) \quad (16)$$

If n is assumed to be 1, and eqn. (16) is combined with the iron couple reactions, then a half order dependence is obtained for case (i) and a first order dependence for case (iii). Case (ii) is given by

$$i_A = 2Fk_{5A}[Cl^-]\{k_{8C}[Fe^{3+}]/(2k_{5A}[Cl^-] + k_{8A}[Fe^{2+}])\}^{0.5} \quad (17)$$

which, at constant and low concentrations of Fe(II), results in a one-half order $[Cl^-]$ dependence. Since Cl^- is specifically adsorbed at the IHP, the change in reaction order with Cl^- concentration is due to the onset of complete coverage. Hence Cl^- may be replaced by the term $[Cl^-]/(1+K[Cl^-])$, where K is the equilibrium constant for Cl^- contact adsorption.

Addition of Cu(II) to leaching solutions

Copper in the cupric form is a well-known activator in the flotation of sphalerite. Copper is exchanged with zinc lattice ions in the solid, and the flotation behaviour is that of CuS. Dutrizac and MacDonald [7] reported that the addition of $CuCl_2$ to the Fe(III) chloride leaching solution increased the rate of reaction, and they accounted for this by proposing that either the CuS film resulted in enhanced galvanic corrosion, or that the cupric ions oxidise the sphalerite and the ferric ions oxidise the resulting cuprous ions. The oxidation of chalcopyrite by cupric chloride has also been proposed, whereas $CuSO_4$ is not an oxidant for chalcopyrite [23].

The dissolution of sphalerite concentrate used in the present study in the presence of $Fe_2(SO_4)_3$ and $CuSO_4$ resulted in diminished rates of reaction. The dissolution kinetics were described by the shrinking-particle model, eqn. (4), and the reaction rate constant, k_r, decreased by a factor of 3.3 on the addition of 0.01 M cupric ion to the 0.5 M Fe(III) leaching solution. Therefore, $CuSO_4$ is not an oxidant for sphalerite, whereas $CuCl_2$ is, behaviour that is similar to that of chalcopyrite.

CONCLUSIONS

The oxidative dissolution of Gamsberg sphalerite is described by an electrochemical mechanism in which the charge transferred from the solid to the oxidant in solution is the rate-controlling step. The electrochemical model has been combined with the knowledge of the solution equilibria to give a more complete view of the dissolution process. It was found that some ionic species in ferric sulphate solutions are inactive while leaching sphalerite. The electroactive complexes in Fe(III) sulphate solutions are $Fe^{3+}(aq)$ and $FeHSO_4^{2+}$, and $FeSO_4^+$ is inactive. The electrochemical mechanism was applied to the results reported in the literature for the leaching of zinc sulphide with Fe(III)

chloride, and successfully yields the order of dependence of the rate on the concentrations of Fe(III), Fe(II) and Cl^-. No complexes were found to be inactive in ferric chloride solutions.

ACKNOWLEDGEMENTS

This paper is published with the permission of the Council for Mineral Technology. The assistance of Dr. M.J. Dry is gratefully acknowledged. The author is indebted to Dr. B. Verbaan and Mr. P. Soal, M.P., for arranging that the author's service as a conscientious objector be done at MINTEK.

REFERENCES

1 Vetter, K., Electrochemical Kinetics — Theoretical and Experimental Aspects, Academic Press, New York, NY, 1967.
2 Jin, Z.-M. and Warren, G.W., Reaction kinetics and electrochemical model for the ferric chloride leaching of sphalerite, in: Tozawa, K. (Ed.), Proc. Int. Symp. on Extractive Metallurgy of Zinc, Min. Metall. Inst. Jpn., Tokyo, 1985, pp. 111-125.
3 Verbaan, B. and Crundwell, F.K., Hydrometallurgy, 16 (1986) 345-359.
4 Crundwell, F.K., M.Sc. Dissertation, University of the Witwatersrand, Johannesburg, 1985.
5 Verbaan, B., Report 2038, National Institute for Metallurgy, Randburg, 1980.
6 Jin, Z.-M., Warren, G.W. and Hunein, H., Metall. Trans., 15B (1984) 5-12.
7 Dutrizac, J.E. and MacDonald, R.J.C., Metall. Trans., 9B (1978) 543-551.
8 Jan, R.J., Hepworth, M.T. and Fox, V.G., Metall. Trans., 7B (1976) 353-361.
9 Dutrizac, J.E. and MacDonald, R.J.C., Miner. Sci. Eng., 6 (1974) 59-100.
10 Wadsworth, M.E., Miner. Sci. Eng., 4 (1972) 36-47.
11 Piao, S.Y. and Tozawa, K., J. Min. Metall. Inst. Jpn., 101 (1985) 795-800.
12 Scott, P.D. and Nicol, M.J., Report 1949, National Institute for Metallurgy, Randburg, 1978.
13 Gelach, J. and Kuzeci, E., Erzmetall, 37 (1984) 261.
14 Guerette, C. and Ghali, E., The anodic dissolution of ZnS-graphite mixture in dilute hydrochloric acid medium, in: Tozawa, K. (Ed.), Proc. Int. Symp. on Extractive Metallurgy of Zinc, Min. Metall. Inst. Jpn., Tokyo, pp. 95-110.
15 Price, D.W. and Warren, G.W., Hydrometallurgy, 15 (1986) 303-324.
16 Richardson, P.E. and O'Dell, C.S., Semiconducting characteristics of galena electrodes, in: Srinivaran, S. and Woods, R. (Eds.), Proc. Int. Symp. on Electrochem. in Mineral and Metal Processing, The Electrochem. Soc., Pennington, 1984, pp. 132-151.
17 Paul, R.L., Nicol, M.J., Diggle, J.W. and Saunders, A.P., Electrochim. Acta, 23 (1978) 625-633.
18 Keys, J.D., Horwood, J.C., Baleshta, T.M., Cabri, C.J. and Harris, D.C., Can. Mineral., 9 (1968) 453-467.
19 Dry, M.J. Ph.D. Thesis, University of the Witwatersrand, Johannesburg 1984.
20 I,T.-P., and Nancollas, G., Anal. Chem., 44 (1972) 1940-1950.
21 Naumov, G.B., Ryzhenko, B.N. and Khadakovsky, I.L., Handbook of Thermodynamic Data, U.S. Department of Commerce, National Technical Information Service, U.S. Geological Survey, Menlo Park, California, 1984.
22 Pitzer, K.S., Roy, R.N. and Sylvester, L.F., J. Amer. Chem. Soc., 99 (1977) 4930-4936.
23 Parker, A.J., Paul, R.L. and Power, G.P., J. Electroanal. Chem., 118 (1981) 305-316; and Aust. J. Chem., 34 (1981) 13.

24 Ashurst, K.G. and Hancock, R.D., National Institute for Metallurgy, Report Nos. 1820 and 1914, Randburg 1977.
25 Butler, J.N., Ionic Equilibrium — A Mathematical Approach, Addison-Wesley, Reading, MA, 1964.
26 Crundwell, F.K. and Verbaan, B., Hydrometallurgy, 17 (1987) 369.
27 Pitzer, K.S., Faraday Trans. II, 68 (1972) 101.